Supporting Information

Design of phase-structure for sodium chloride solid electrolytes with outstanding performance: First-principles approach†

Yuxiang Lian,[a] Musheng Wu,[a,*] Bo Xu,[a] Bing He,[a] Gang Liu,[a] Jing Shi, [a] Qingqiang Kuang,[a] Hewen Wang,[b] and Chuying Ouyang [a,*]

[a]*College of Physics, Communication and Electronics, Laboratory of Computational Materials Physics, Jiangxi Normal University, Nanchang 330022, China*.

[b]*College of Chemistry and Chemical Engineering, Hubei Key Laboratory for Processing and Application of Catalytic Materials, Huanggang Normal University, Huanggang 438000, China.*

*Corresponding Author E-mail: smwu@jxnu.edu.cn; cyouyang@jxnu.edu.cn.

1. Detailed calculations

For primitive cell optimizations and elastic property calculations of Na_3XCl_6 (X=In, Sc), a Monkhorst-Pack[1] *k*-point grid with a density of 1 point per 0.02 $Å^{-3}$ in the Brillouin zone was sampled. For the density of states (DOS) calculations of Na_3XCl_6 (X=In, Sc), a density of 1 point per 0.003 $Å^{-3}$ in the Brillouin zone was used. The convergence thresholds of total energy and the final force on each atom were less than 1×10^{-6} eV and 0.01 eV/Å, respectively. The Gaussian smearing method with a smearing width of 0.05 eV was used. The Heyd-Scuseria-Erznerhof (HSE06)[2] hybrid functional was used to calculate the DOS of Na_3XCl_6 (X=In, Sc), because hybrid Hartree-Fock/DFT approaches[3] has been proven more reliable than the GGA-PBE functional in terms of band gaps.

To examine the dynamical stabilities of *C2/m*- and $p\bar{3}m1$-Na_3XCl_6 (X=In, Sc) predicted in this work, The frozen-phonon method was adopted to calculate the force constant matrix and the phonon dispersion spectrum by using PHONOPY package.[4] The CALYPSO software[5] was used to search the different atomic configurations in Na_3InCl_6 and Na_3ScCl_6 primitive cells in order to obtain accurately the ground-state structures of both.

To investigate the probability distributions of Na-ions, the bond valence site energy (BVSE) method, which has been widely used in crystal chemistry for quickly assessing the plausibility of crystal structure and investigating preferred ionic migration pathways,[6] was performed by using the soft-BV software.[7] The Na bond valence site energies were calculated by setting a dense grid with a resolution of 0.1 Å, followed by the identification of the corresponding Na-ion diffusion

channels.

Furthermore, to further uncover Na-ion kinetics under dynamic conditions, we also performed AIMD simulation and climbing-image nudged elastic band (CI-NEB) method[8] to study Na-ion conductivities and migration energy barriers. The AIMD simulations were performed by a Nosé-Hoover thermostat[9] in a statistical ensemble of fixed particle number, volume, and temperature conditions (NVT) conditions. 2×1×2 Na_3InCl_6 and Na_3ScCl_6 supercells (80 atoms for *c2m* and 120 atoms for $p\bar{3}m1$) were chosen for a **k**-point sampling at the Γ-point. A Verlet algorithm was integrated with Newton's equations of motion. The time-step of the simulations was set to 2 fs and 15000 steps were performed after a 2 ps pre-equilibrium run at temperatures ranging from 500 to 900 K. Statistical analyses of the AIMD simulations were conducted using Python Materials Genomics (pymatgen)[10] library and the pymatgen-diffusion add-on package[11] in order to understand the Na-ion diffusion behaviors.

The self-diffusion coefficient (D) of Na^+, Cl^- and In/Sc^{3+} can be described by a time-dependent mean-square displacement (MSD):

$$D = \lim_{t\to\infty} \frac{MSD(t)}{2dt} , \quad \text{(S1)}$$

where t is time, and d is the dimensionality of the system. The MSD(t) can be described as

$$\mathrm{MSD}(t) = <\delta r^2(t)> = \frac{1}{N}\frac{1}{n}\sum_{j=0}^{n}\sum_{i=0}^{N}[r_i(t_{0j}+t) - r_i(t_{0j})]^2 , \quad \text{(S2)}$$

where N is the total number of ions in the system, n is the number of time origins, t_{0j} is the initial time step originating at time j, and $r_i(t)$ is the displacement of the ith ion at time t.[12] The D was finally attained from the slope of the MSD vs. time plot for each temperature, from which an Arrhenius plot was obtained which yielded the activation energy.

The ionic conductivity (σ) is correlated with the above D by the Nernst-Einstein equation:

$$\sigma = \frac{N_{ion} q^2 D}{H_R k_B T} , \quad \text{(S3)}$$

where N_{ion} and q are the number density and charge of the mobile ion of interest, respectively, k_B is the Boltzmann's constant, T is the absolute temperature, H_R is the Haven ratio between the tracer diffusivity D^* and charge diffusivity D_σ: $H_R = D^*/D_\sigma$, and was taken as 1 in the present study.[13]

2. Geometries and stabilities

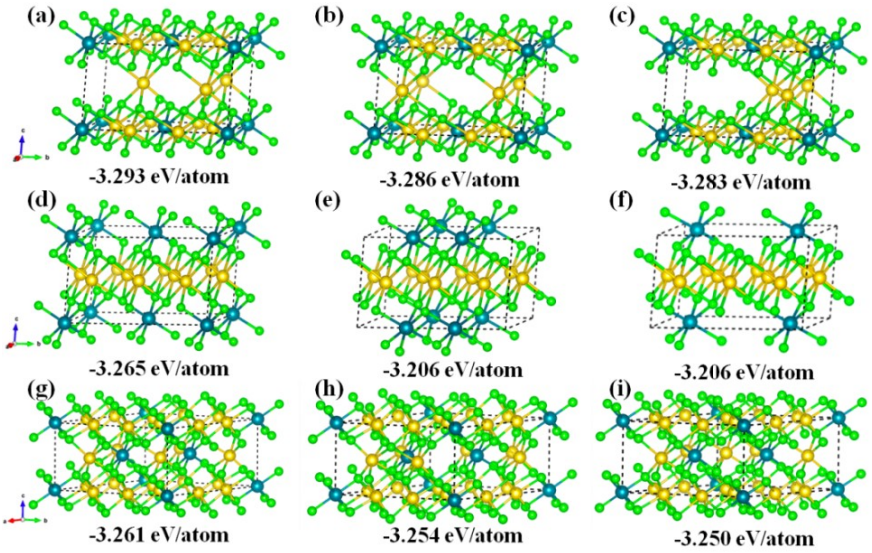

Fig. S1 The atomic configurations with the lowest energy and next in energy of (a)-(c) *c2m*-NIC derived from Li_3ScCl_6,[14] (d)-(f) *c2m*-NIC derived from Li_3InCl_6,[15] (g)-(i) *p3m1*-NIC derived from Li_3YCl_6.[16] The energies are marked below each structure diagram.

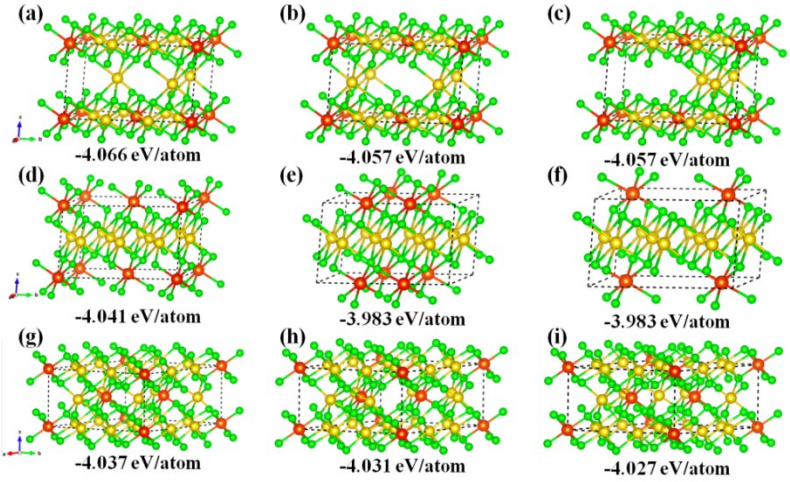

Fig. S2 The atomic configurations with the lowest energy and next in energy of (a)-(c) *c2m*-NSC derived from Li_3ScCl_6,[14] (d)-(f) *c2m*-NSC derived from Li_3InCl_6,[15] (g)-(i) *p3m1*-NSC derived from Li_3YCl_6.[16] The energies are marked below each structure diagram.

Table S1. Structure information of the *c2m*-NXC and *p3m1*-NXC with corresponding atomic positions.

c2m-NIC	*c2m*-NSC	*p3m1*-NIC	*p3m1*-NSC
a=7.01, *b*=11.84, *c*=7.03 α=90.0 β=109.2 γ=90.0 an unit-cell Vol=551.4 Å^3	*a*=7.01, b=11.81, c=7.00 α=90.0 β=109.8 γ=90.0 an unit-cell Vol=545.3 Å^3	a=11.60, b=11.60, c=6.64 α=90.0 β=90.0 γ=120.0 an unit-cell Vol=774.7 Å^3	a=11.52, b=11.52, c=6.60 α=90.0 β=90.0 γ=120.0 an unit-cell Vol=758.8 Å^3
Na1 (0.500, 0.834, 0.000) Na2 (0.000, 0.334, 0.000) Na3 (0.500, 0.164, 0.000)	Na1 (0.500, 0.835, 0.000) Na2 (0.000, 0.335, 0.000) Na3 (0.500, 0.164, 0.000)	Na1 (0.348, 0.348, 0.000) Na2 (0.656, 0.656, 0.000) Na3 (0.651, 0.000, 0.000)	Na1 (0.348, 0.348, 0.000) Na2 (0.656, 0.656, 0.000) Na3 (0.651, 0.000, 0.000)

Na4 (0.000, 0.664, 0.000)	Na4 (0.000, 0.664, 0.000)	Na4 (0.343, 0.000, 0.000)	Na4 (0.343, 0.000, 0.000)
Na5 (0.000, 0.833, 0.500)	Na5 (0.000, 0.829, 0.500)	Na5 (0.000, 0.651, 0.000)	Na5 (0.000, 0.651, 0.000)
Na6 (0.500, 0.333, 0.500)	Na6 (0.500, 0.329, 0.500)	Na6 (0.000, 0.343, 0.000)	Na6 (0.000, 0.343, 0.000)
In1 (0.000, 0.003, 0.000)	Sc1 (0.000, 0.004, 0.000)	Na7 (0.307, 0.000, 0.500)	Na7 (0.307, 0.000, 0.500)
In2 (0.500, 0.503, 0.000)	Sc2 (0.500, 0.504, 0.000)	Na8 (0.000, 0.307, 0.500)	Na8 (0.000, 0.307, 0.500)
Cl1 (0.217, 0.848, 0.226)	Cl1 (0.216, 0.850, 0.225)	Na9 (0.692, 0.692, 0.500)	Na9 (0.692, 0.692, 0.500)
Cl2 (0.717, 0.348, 0.226)	Cl2 (0.716, 0.350, 0.225)	In1 (0.000, 0.000, 0.000)	Sc1 (0.000, 0.000, 0.000)
Cl3 (0.782, 0.848, 0.773)	Cl3 (0.783, 0.850, 0.774)	In2 (0.333, 0.666, 0.499)	Sc2 (0.333, 0.666, 0.499)
Cl4 (0.282, 0.348, 0.773)	Cl4 (0.283, 0.350, 0.774)	In3 (0.666, 0.333, 0.500)	Sc3 (0.666, 0.333, 0.500)
Cl5 (0.770, 0.157, 0.781)	Cl5 (0.769, 0.157, 0.781)	Cl1 (0.103, 0.892, 0.786)	Cl1 (0.102, 0.894, 0.786)
Cl6 (0.270, 0.657, 0.781)	Cl6 (0.269, 0.657, 0.781)	Cl2 (0.892, 0.103, 0.213)	Cl2 (0.894, 0.102, 0.213)
Cl7 (0.229, 0.157, 0.218)	Cl7 (0.230, 0.157, 0.218)	Cl3 (0.107, 0.211, 0.786)	Cl3 (0.105, 0.207, 0.786)
Cl8 (0.729, 0.657, 0.218)	Cl8 (0.730, 0.657, 0.218)	Cl4 (0.896, 0.788, 0.213)	Cl4 (0.897, 0.792, 0.213)
Cl9 (0.773, 0.997, 0.219)	Cl9 (0.776, 0.997, 0.218)	Cl5 (0.788, 0.896, 0.786)	Cl5 (0.792, 0.897, 0.786)
Cl10 (0.273, 0.497, 0.219)	Cl10 (0.276, 0.497, 0.218)	Cl6 (0.211, 0.107, 0.213)	Cl6 (0.207, 0.105, 0.213)
Cl11 (0.226, 0.997, 0.780)	Cl11 (0.223, 0.997, 0.781)	Cl7 (0.230, 0.772, 0.275)	Cl7 (0.232, 0.771, 0.275)
Cl12 (0.726, 0.497, 0.780)	Cl12 (0.723, 0.497, 0.781)	Cl8 (0.772, 0.230, 0.724)	Cl8 (0.771, 0.232, 0.724)
		Cl9 (0.227, 0.457, 0.275)	Cl9 (0.228, 0.461, 0.275)
		Cl10 (0.769, 0.542, 0.724)	Cl10 (0.767, 0.538, 0.724)
		Cl11 (0.542, 0.769, 0.275)	Cl11 (0.538, 0.767, 0.275)
		Cl12 (0.457, 0.227, 0.724)	Cl12 (0.461, 0.228, 0.724)
		Cl13 (0.447, 0.571, 0.724)	Cl13 (0.445, 0.573, 0.723)
		Cl14 (0.571, 0.447, 0.275)	Cl14 (0.573, 0.445, 0.276)
		Cl15 (0.428, 0.876, 0.724)	Cl15 (0.426, 0.872, 0.723)
		Cl16 (0.552, 0.123, 0.275)	Cl16 (0.554, 0.127, 0.276)
		Cl17 (0.123, 0.552, 0.724)	Cl17 (0.127, 0.554, 0.723)
		Cl18 (0.876, 0.428, 0.275)	Cl18 (0.872, 0.426, 0.276)

The phase stability of the investigated phase was evaluated using the decomposition energy (E_{decomp}),

$$E_{decomp} = E_{eq}(C) - E(NXC), \quad \text{(S4)}$$

where $E_{eq}(C)$ indicates the total energy of the phase equilibria at the composition C determined from the compositional phase diagram, $E(NXC)$ is the total energy of the solid electrolyte NXC of a given phase. For instance, the phase equilibria at the composition NaCl and $InCl_3$ ($NaScCl_4$) can be described as the following reaction:

$$Na_3InCl_6 \rightarrow 3NaCl + InCl_3, \quad \text{(S5)}$$

$$Na_3ScCl_6 \rightarrow 2NaCl + NaScCl_4, \quad \text{(S6)}$$

$E_{eq}(C)$ is the total energies of NaCl and $InCl_3$/$NaScCl_4$, E(NXC) is the energies of a given phase NIC or NSC.

Table S2. Energy above the hull (E_{hull}) of all phases for Na-In-Cl ternary system

Materials ID	Composition	Space Group	E_{hull} (meV/atom)
NIC-in this work	Na_3InCl_6	C2/m	0
NIC-in this work	Na_3InCl_6	$P\bar{3}m1$	0
NIC-in this work	Na_3InCl_6	$P\bar{3}1c$	0
mp-1113312	Na_3InCl_6	$Fm\bar{3}m$	146.03
mp-1186081	Na	$I\bar{4}3m$	0
mp-1184502	In	$R\bar{3}m$	0
mp-1008394	Cl_2	Cmce	0
mp-20628	NaIn	$Fd\bar{3}m$	0
mp-31430	Na_2In	$C222_1$	0
mp-976589	$NaIn_3$	$Pm\bar{3}m$	0
mp-28730	In_7Cl_9	$Pa\bar{3}$	0
mp-23276	InCl	$P2_13$	0
mp-1212122	$InCl_2$	Pnna	0
mp-862983	$InCl_3$	$P6_3/mmc$	0
mp-22862	NaCl	$Fm\bar{3}m$	0
mp-1189265	$NaCl_3$	Pnma	0
mp-1080771	$NaCl_7$	$Pm\bar{3}$	0

Table S3. Energy above the Hull (E_{hull}) of all phases for Na-Sc-Cl ternary system

Materials ID	Composition	Space Group	E_{hull} (meV/atom)
NSC-in this work	Na_3ScCl_6	C2/m	0
NSC-in this work	Na_3ScCl_6	$P\bar{3}m1$	22.11
NSC-in this work	Na_3ScCl_6	$P2_1/n$	1.31
mp-1189516	Na_3ScCl_6	$P2_1/c$	1.31
mp-1189518	Na_3ScCl_6	$Fm\bar{3}m$	117.30
mp-29432	$NaScCl_4$	Pbcn	0
mp-1186081	Na	$I\bar{4}3m$	0
mp-1184502	In	$R\bar{3}m$	0
mp-1008394	Cl_2	Cmce	0
mp-27513	Sc_7Cl_{10}	C2/m	0
mp-23309	$ScCl_3$	$R\bar{3}$	0
mp-542449	Sc_5Cl_8	C2/m	0
mp-22862	NaCl	$Fm\bar{3}m$	0
mp-1189265	$NaCl_3$	Pnma	0
mp-1080771	$NaCl_7$	$Pm\bar{3}$	0

3. Electrochemical stabilities

To study the electrochemical stability of NXC, the grand potential phase diagrams[17] were formulated to identify the phase equilibria with respect to open Na species (μ_{Na}) at a given applied potential φ. The grand potential phase diagram identifies the phase equilibria of a given phase with the composition $C_{eq}([C_{Na},C_{In/Sc},C_{Cl}])$ at φ. The applied potential φ is defined as,

$$\mu_{Na}(\varphi) = \mu_{Na}^{0} - e\varphi, \quad \text{(S7)}$$

where μ_{Na}^{0} is the chemical potential of Na metal. The electrochemical window of the phase was estimated as the range of φ, where the phase is neither oxidized nor reduced. The energy of decomposition reaction at a given φ ($\Delta E_D(\varphi)$) is determined using,

$$\Delta E_D(\varphi) = E_{eq}\left(C_{eq}([C_{Na},C_{In/Sc},C_{Cl}],\varphi)\right) - E(NXC) - n_{Na}\mu_{Na}(\varphi), \quad \text{(S8)}$$

where $E_{eq}\left(C_{eq}([C_{Na},C_{In/Sc},C_{Cl}],\varphi)\right)$ is the phase equilibria energy from the composition system $C_{eq}([C_{Na},C_{In/Sc},C_{Cl}])$ at φ, $E(NXC)$ is the energy of NXC at a given phase, n_{Na} is the number of Na exchanged between NXC and $C_{eq}([C_{Na},C_{In/Sc},C_{Cl}])$ during sodiation or desodiation. According to eqn. (S8), the decomposition energies of the phase equilibria with all relevant compositions for NXC of considered phases were listed in Tables S4 and S5.

Table S4. Calculated phase equilibria for the NIC at applied potential φ.

Potential φ ref to Na/Na$^+$ (V)			μ_{Na} ref to Na metal (eV)			n_{Na} per formula	Phase equilibria
p31c	*c2m*	*p3m1*	*p31c*	*c2m*	*p3m1*		
1.33	1.34	1.40	-1.33	-1.34	-1.40	5	NaCl, $NaIn_2$
1.64	1.65	1.73	-1.64	-1.65	-1.73	4	NaCl, NaIn
2.09	2.12	2.22	-2.09	-2.12	-2.22	3	NaCl, In
2.09	2.15	2.45	-2.09	-2.15	-2.45	1	NaCl, $InCl_2$
2.14	2.18	2.35	-2.14	-2.18	-2.35	1.71	NaCl, In_7Cl_9
2.15	2.18	2.33	-2.15	-2.18	-2.33	2	NaCl, InCl
						0	Na_3InCl_6
4.07	4.04	3.89	-4.07	-4.04	-3.89	-2	$NaCl_3$, $InCl_3$
4.44	4.42	4.32	-4.44	-4.42	-4.32	-3	$InCl_3$, Cl_2

Table S5. Calculated phase equilibria for the NSC at applied potential φ

Potential φ ref to Na/Na$^+$ (V)			μ_{Na} ref to Na metal (eV)			n_{Na} per formula	Phase equilibria
P21n	*c2m*	*p3m1*	*P21n*	*c2m*	*p3m1*		

0.79	0.77	0.86	-0.79	-0.77	-0.86	3	Sc, NaCl
0.85	0.82	0.99	-0.85	-0.82	-0.99	1.57	Sc_7Cl_{10}, NaCl
0.85	0.82	1.00	-0.85	-0.82	-1.00	1.5	Sc_5Cl_8, Sc_7Cl_{10}, NaCl
0.86	0.83	1.01	-0.86	-0.83	-1.01	1.4	Sc_5Cl_8, NaCl
						0	Na_3ScCl_6
3.76	3.79	3.66	-3.76	-3.79	-3.66	-2	$NaCl_3$, $ScCl_3$
4.23	4.25	4.16	-4.23	-4.25	-4.16	-3	Cl_2, $ScCl_3$

4. Interfacial stabilities with cathode

In this work, the interface (C_{inter}) was first considered as a pseudo-binary[18] of solid electrolyte NXC and the cathode, which has a composition C_{NXC} and C_{cath}, expressed as follows：

$$C_{inter}(C_{NXC},C_{cath},x) = x \cdot C_{NXC} + (1-x) \cdot C_{cath}, \quad \text{(S9)}$$

where C_{NXC} and C_{cath} are the compositions (normalized to one atom per formula) of NXC and cathode materials, respectively, and x is the molar fraction of the NXC which varies from 0 to 1. The energy of the interface pseudo-binary can be expressed as:

$$E_{inter}(NXC, cathode, x) = x \cdot E(NXC) + (1-x) \cdot E(cathode), \quad \text{(S10)}$$

the E_{interf} was set to a linear combination of the energies of NXC ($E(NXC)$) and cathode ($E(cathode)$). Then the decomposition reaction energy ($\Delta E_D(x)$) of the interface pseudo-binary was calculated as：

$$\Delta E_D(x) = E_{eq}\big(C_{inter}(C_{NXC},C_{cath},x)\big) - E_{inter}(NXC,cath,x), \quad \text{(S11)}$$

where E_{eq} is the phase equilibria energy from composition C_{inter}, $\Delta E_D(x)$ includes the decomposition energy E_{decomp} from eqn. (S1) if the NXC or the cathode is not thermodynamically stable. Next, the mutual reaction energy ($\Delta E_D^{mut}(x)$) between phase equilibria of NXC and cathode was identified as:

$$\Delta E_D^{mut}(x) = \Delta E_D(x) - x \cdot E_{decomp}(NXC) - (1-x) \cdot E_{decomp}(cath), \quad \text{(S12)}$$

since the phase equilibria and the reaction energies vary with the pseudo-binary composition, the minimum of the mutual reaction energy was defined as:

$$\Delta E_{D,min}^{mut} = \min_{x \in (0,1)} \left[\Delta E_D^{mut}(x)\right], \quad \text{(S13)}$$

Table S6. Phase equilibria and the calculated minimum mutual reaction energies $\Delta E_{D,min}^{mut}$ of the interfaces between *p3m1*-NIC and currently used common cathodes.

Molar Fraction	Reaction Equation	$\Delta E_{D,min}^{mut}$ (eV/atom)
Cathode - $NaCoO_2$		
1.000	$Na_3InCl_6 \rightarrow Na_3InCl_6$	0.000
0.229	0.229 Na_3InCl_6 + 0.771 $NaCoO_2 \rightarrow$ 0.086 $Na(CoO_2)_3$ +	-0.095

	0.171 Co_3O_4 + 0.114 In_2O_3+ 1.371 NaCl	
0.200	0.2 Na_3InCl_6 + 0.8 $NaCoO_2$ → 0.15 Co_3O_4 + 0.05 $Na_4(CoO_2)_7$ + 0.1 In_2O_3 + 1.2 NaCl	-0.089
0.167	0.167 Na_3InCl_6 + 0.833 $NaCoO_2$ → 0.083 $Na_4(CoO_2)_7$ + 0.083 In_2O_3 + NaCl + 0.25 CoO	-0.080
0.118	0.118 Na_3InCl_6 + 0.882 $NaCoO_2$ → 0.176 $Na_3(CoO_2)_4$ + 0.059 In_2O_3 + 0.706 NaCl + 0.176 CoO	-0.061
0.000	$NaCoO_2$ → $NaCoO_2$	-0.000
Cathode - $NaCrO_2$		
1.000	Na_3InCl_6 → Na_3InCl_6	0.000
0.250	0.25 Na_3InCl_6 + 0.75 $NaCrO_2$ → 0.125 In_2O_3 + 0.375 Cr_2O_3 + 1.5 NaCl	-0.101
0.000	$NaCrO_2$ → $NaCrO_2$	0.000
Cathode - $NaFePO_4$		
1.000	Na_3InCl_6 → Na_3InCl_6	0.000
0.250	0.25 Na_3InCl_6 + 0.75 $NaFePO_4$ → 0.375 Fe_2PClO_4 + 0.125 $Na_3In_2(PO_4)_3$ + 1.125 NaCl	-0.014
0.000	$NaFePO_4$ → $NaFePO_4$	-0.000
Cathode - $Na_3V_2(PO_4)_3$		
1.000	Na_3InCl_6 → Na_3InCl_6	0.000
0.400	0.4 Na_3InCl_6 + 0.6 $Na_3V_2(PO_4)_3$ → 1.2 VPO_4 + 0.2 $Na_3In_2(PO_4)_3$ + 2.4 NaCl	-0.026
0.286	0.286 Na_3InCl_6 + 0.714 $Na_3V_2(PO_4)_3$ → 0.857 $NaVP_2O_7$ + 0.143 $Na_3In_2(PO_4)_3$ + 1.714 NaCl + 0.286 V_2O_3	-0.024
0.231	0.231 Na_3InCl_6 + 0.769 $Na_3V_2(PO_4)_3$ → 0.923 $NaVP_2O_7$ + 0.231 $Na_3In(PO_4)_2$ + 1.385 NaCl + 0.308 V_2O_3	-0.019
0.000	$Na_3V_2(PO_4)_3$ →$Na_3V_2(PO_4)_3$	-0.000

Table S7. Phase equilibria and the calculated minimum mutual reaction energies $\Delta E_{D,min}^{mut}$ of the interfaces between *p3m1*-NSC and currently used common cathodes.

Molar Fraction	Reaction Equation	$\Delta E_{D,min}^{mut}$ (eV/atom)
Cathode - $NaCoO_2$		
1.000	Na_3ScCl_6 →Na_3ScCl_6	0.000
0.308	0.308 Na_3ScCl_6 + 0.692 $NaCoO_2$ → 0.115 $NaCl_3$ + 0.231 Co_3O_4 + 1.5 NaCl + 0.154 Sc_2O_3	-0.104
0.229	0.229 Na_3ScCl_6 + 0.771 $NaCoO_2$ → 0.086 $Na(CoO_2)_3$ + 0.171 Co_3O_4 + 1.371 NaCl + 0.114 Sc_2O_3	-0.122
0.200	0.2 Na_3ScCl_6 + 0.8 $NaCoO_2$ → 0.15 Co_3O_4 + 0.05 $Na_4(CoO_2)_7$ + 1.2 NaCl + 0.1 Sc_2O_3	-0.113

0.167	0.167 Na_3ScCl_6 + 0.833 $NaCoO_2$ → 0.083 $Na_4(CoO_2)_7$ + 0.25 CoO + NaCl + 0.083 Sc_2O_3	-0.100
0.118	0.118 Na_3ScCl_6 + 0.882 $NaCoO_2$ → 0.176 $Na_3(CoO_2)_4$ + 0.176 CoO + 0.706 NaCl + 0.059 Sc_2O_3	-0.076
0.000	$NaCoO_2$ → $NaCoO_2$	-0.000
Cathode - $NaCrO_2$		
1.000	Na_3ScCl_6 →Na_3ScCl_6	0.000
0.571	0.571 Na_3ScCl_6 + 0.429 $NaCrO_2$ → 0.429 Na_3CrCl_6 + 0.286 Sc_2O_3 + 0.857 NaCl	-0.059
0.250	0.25 Na_3ScCl_6 + 0.75 $NaCrO_2$ → 0.125 Sc_2O_3 + 0.375 Cr_2O_3 + 1.5 NaCl	-0.129
0.000	$NaCrO_2$ → $NaCrO_2$	-0.000
Cathode - $NaFePO_4$		
1.000	Na_3ScCl_6 →Na_3ScCl_6	0.000
0.333	0.333 Na_3ScCl_6 + 0.667 $NaFePO_4$ → 0.333 $ScPO_4$ + 0.333 Fe_2PClO_4 + 1.667 NaCl	-0.056
0.250	0.25 Na_3ScCl_6 + 0.75 $NaFePO_4$ → 0.375 Fe_2PClO_4 + 0.125 $Na_3Sc_2(PO_4)_3$ + 1.125 NaCl	-0.046
0.000	$NaFePO_4$ → $NaFePO_4$	-0.000
Cathode - $Na_3V_2(PO_4)_3$		
1.000	Na_3ScCl_6 →Na_3ScCl_6	0.000
0.750	0.75 Na_3ScCl_6 + 0.25 $Na_3V_2(PO_4)_3$ → 0.75 $ScPO_4$ + 0.25 VCl_2 + 0.25 VCl_4 + 3 NaCl	-0.035
0.740	0.74 Na_3ScCl_6 + 0.26 $Na_3V_2(PO_4)_3$ → 0.74 $ScPO_4$ + 0.04 VP + 0.32 VCl_4 + 3 NaCl + 0.16 VClO	-0.036
0.500	0.5 Na_3ScCl_6 + 0.5 $Na_3V_2(PO_4)_3$ → VPO_4 + 0.5 $ScPO_4$ + 3 NaCl	-0.057
0.400	0.4 Na_3ScCl_6 + 0.6 $Na_3V_2(PO_4)_3$ → 0.2 $Na_3Sc_2(PO_4)_3$ + 1.2 VPO_4 + 2.4 NaCl	-0.046
0.286	0.286 Na_3ScCl_6 + 0.714 $Na_3V_2(PO_4)_3$ → 0.143 $Na_3Sc_2(PO_4)_3$ + 0.857 $NaVP_2O_7$ + 0.286 V_2O_3 + 1.714 NaCl	-0.040
0.000	$Na_3V_2(PO_4)_3$ →$Na_3V_2(PO_4)_3$	-0.000

5. Mechanical and thermal properties

Table S8. The elastic constants (C) of all considered NXC in this work, unit: GPa.

elastic constants	*c2m*-NIC	*c2m*-NSC	*p3m1*-NIC	*p3m1*-NSC	*p31c*-NIC	*p21n*-NSC
C_{11}	26.48	25.54	35.62	37.46	28.39	32.36
C_{12}	8.83	8.68	16.34	16.06	14.34	15.77
C_{13}	4.63	4.87	12.08	12.37	12.39	11.44
C_{14}	-	-	-0.15	-0.25	-0.03	-

C_{15}	-0.97	-0.62	-	-	-	1.48
C_{22}	32.20	32.62	-	-	-	41.92
C_{23}	3.99	4.65	-	-	-	11.80
C_{25}	-0.46	0.14	-	-	-	2.67
C_{33}	14.40	15.04	32.28	33.44	30.82	33.48
C_{35}	-2.45	-1.63	-	-	-	-2.93
C_{44}	3.10	4.18	10.09	10.66	7.48	9.82
C_{46}	-0.18	0.12	-	-	-	0.24
C_{55}	5.55	5.54	-	-	-	7.92
C_{66}	10.05	9.96	-	-	-	12.14

The lattice thermal conductivity (κ_L) can be defined as the following expression:

$$\kappa_L = A\frac{\bar{M}\theta_D^3\delta}{\gamma^2 n^{2/3} T}, \quad \text{(S14)}$$

here n is the number of atoms per molecule, δ [unit: m] is the cube root of the average volume occupied by one atom, $\bar{M}$ [kg/mol] is the mean atomic weight of all the constituent atoms, T [K] is the absolute temperature, θ_D [K] is the acoustic Debye temperature which can be determined by the elastic constants using eqns. (S15)-(S17), γ is the acoustic Grüneisen parameter obtained by using eqn. (S18), which is confirmed to be in good agreement with the quasiharmonic phonon-calculated results for the six-coordinated structures.[19] A [W·mol/(kg·m^2·K^3)] is a coefficient determined by γ according to eqn. (S19).

$$\theta_D = \frac{h}{k_B}\left[\frac{3n}{4\pi}\left(\frac{N_A\rho}{M}\right)\right]^{\frac{1}{3}} v_m, \quad \text{(S15)}$$

$$v_m = \left[\frac{1}{3}\left(\frac{1}{v_l^3} + \frac{2}{v_s^3}\right)\right]^{-\frac{1}{3}}, \quad \text{(S16)}$$

$$v_l = \sqrt{\frac{B + \frac{4}{3}G}{\rho}}, \quad v_s = \sqrt{\frac{G}{\rho}}, \quad \text{(S17)}$$

$$\gamma = \frac{9{v_l}^2 - 12{v_s}^2}{2{v_l}^2 + 4{v_s}^2}, \quad \text{(S18)}$$

$$A = \frac{2.43 \times 10^7 \times \gamma^2}{0.228 - 0.514\gamma + \gamma^2}.$$

(S19)

Where k_B [J/K] and h [J·S] are the Boltzmann's constant and the Plank constant respectively, N_A [1/mol] is the Avogadro's number, ρ [kg/m^3] is the atomic density in the primitive unit cell, M is the total atomic weight of the primitive unit cell, v_m [m/s] is the average sound velocity, v_L and v_s are the longitude and shear wave velocities, and here for B and G in units of Pa.

6. Sodium-ion transport properties

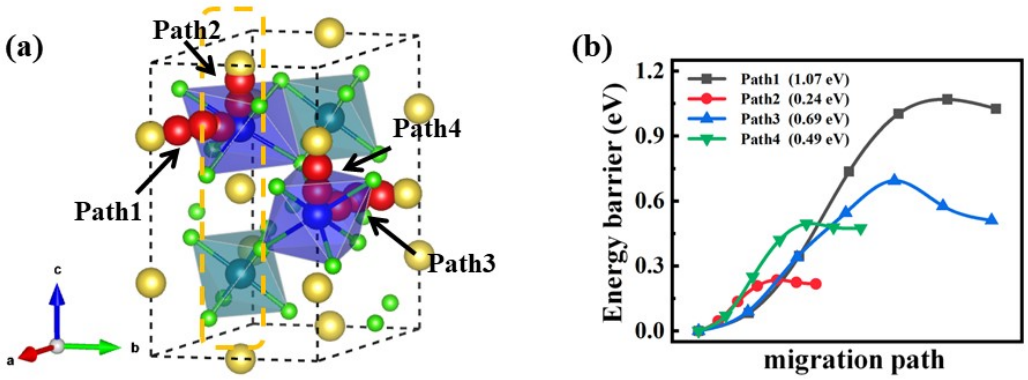

Fig. S3. (a) Schematic drawing of single Na-ion migration pathway in *P31c*-NIC. (b) Energy profile along different migration pathways of Path1, Path2, and Path3. The red spheres represent transition Na ions. The blue octahedron represents the intrinsic Na-ion vacancy.

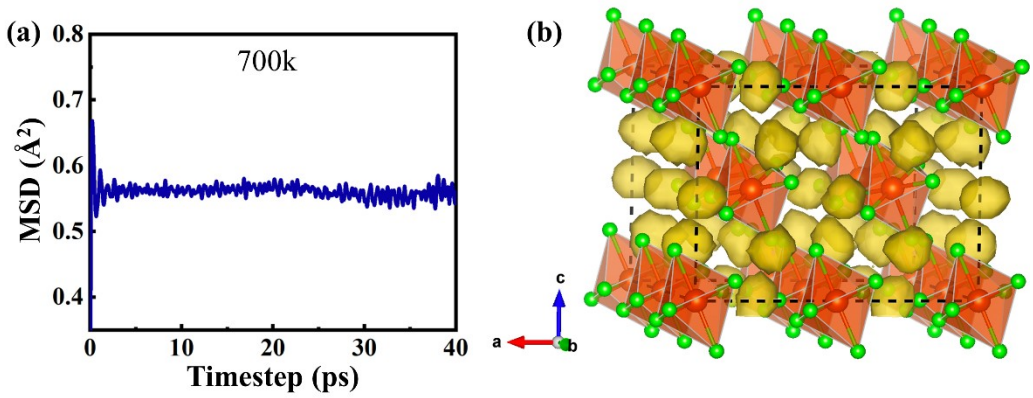

Fig. S4. (a) Na-ion MSD of *p21n*-NSC during 40 ps at 700 K. (b) Isosurfaces of the Na-ion probability densities (yellow) from 40 ps AIMD calculation at 700 K. Corresponding density distribution at 700 K. The isosurface value is set to be 0.0009 e/Bohr.

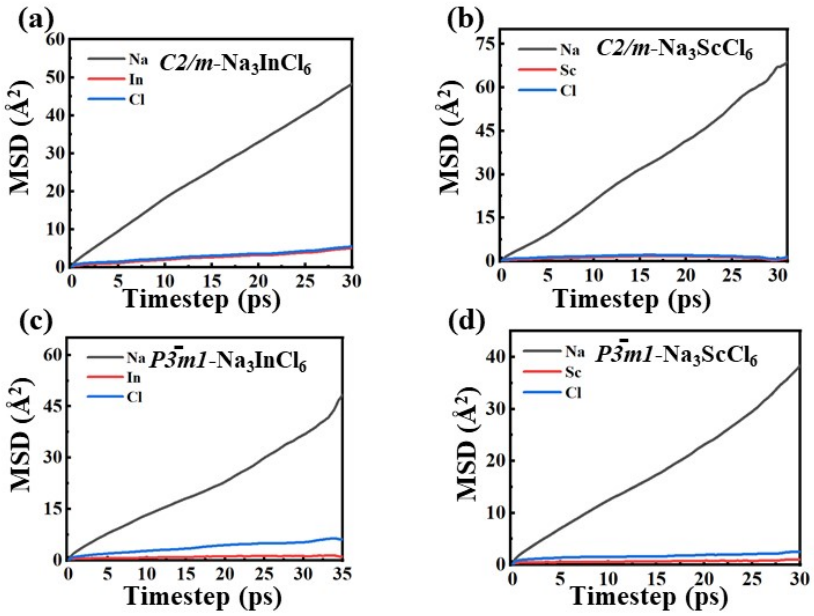

Fig. S5. The MSD of Na, In/Sc and Cl in (a) *c2m*-NIC, (b) *c2m*-NIC, (c) *p3m1*-NIC, and (d) *p3m1*-NSC versus time during the AIMD simulation at 800 K.

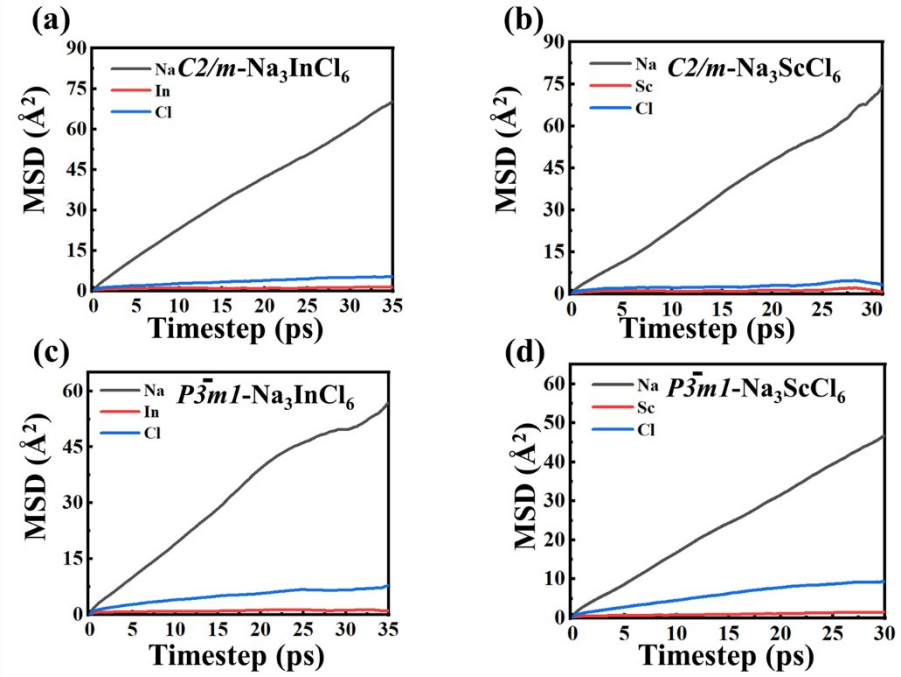

Fig. S6. The MSD of Na, In/Sc and Cl in (a) *c2m*-NIC, (b) *c2m*-NIC, (c) *p3m1*-NIC, and (d) *p3m1*-NSC versus time during the AIMD simulation at 900 K.

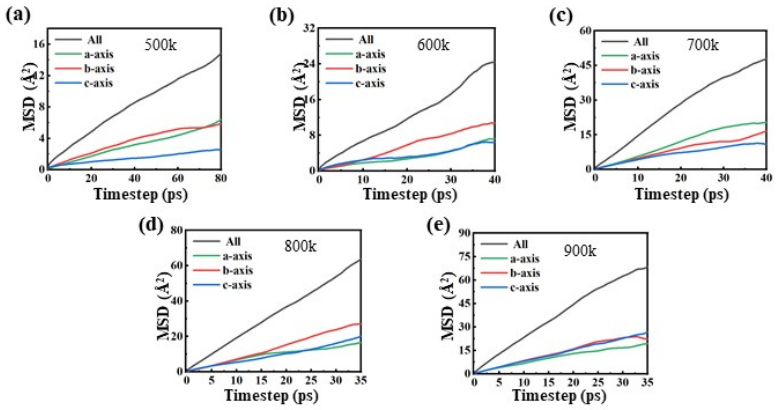

Fig. S7. MSD of Na ions in *c2m*-NIC along different directions as a function of time at different temperatures (500, 600, 700, 800, 900 K).

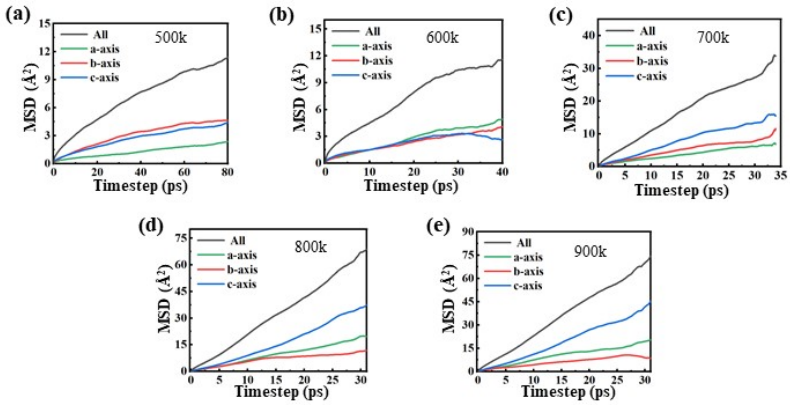

Fig. S8. MSD of Na ions in *c2m*-NSC along different directions as a function of time at different temperatures (500, 600, 700, 800, 900 K).

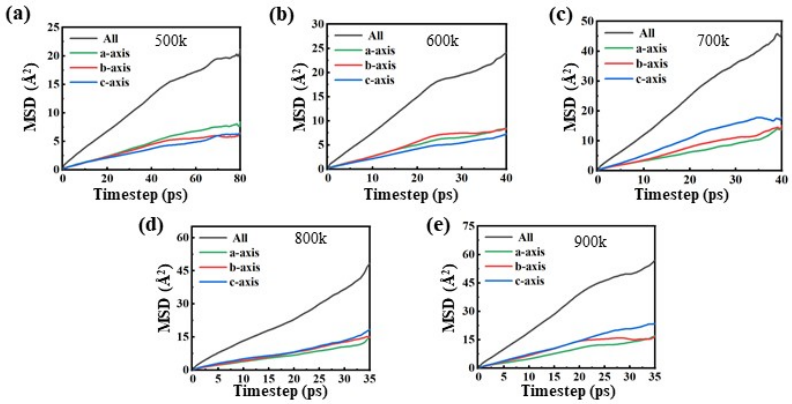

Fig. S9. MSD of Na ions in *p3m1*-NIC along different directions as a function of time at different temperatures (500, 600, 700, 800, 900 K).

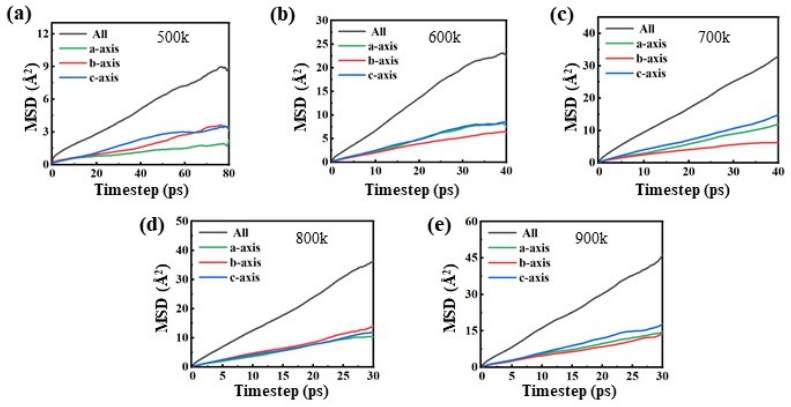

Fig. S10. MSD of Na ions in *p3m1*-NSC along different directions as a function of time at different temperatures (500, 600, 700, 800, 900 K).

References

1. H. J. Monkhorst and J. D. Pack, *Phys. Rev. B*, 1976, **13**, 5188-5192.
2. A. V. Krukau, O. A. Vydrov, A. F. Izmaylov and G. E. Scuseria, *J. Chem. Phys.*, 2006, **125**, 224106.
3. Y. S. Kim, K. Hummer and G. Kresse, *Phys. Rev. B*, 2009, **80**, 035203.
4. A. Togo and I. Tanaka, *Scripta Mater.*, 2015, **108**, 1-5.
5. Y. C. Wang, J. Lv, L. Zhu and Y. M. Ma, *Phys. Rev. B*, 2010, **82**, 094116.
6. S. Adams, *Solid State Ionics*, 2000, **136–137**, 1351–1361.
7. H. Chen, L. L. Wong and S. Adams, *Acta Crystallogr. Sect. B*, 2019, **75**, 18-33.
8. G. Henkelman, B. P. Uberuaga and H. Jónsson, *J. Chem. Phys.*, 2000, **113**, 9901-9904.
9. W. G. Hoover, *Phys. Rev. A*, 1985, **31**, 1695-1697.
10. S. P. Ong, W. D. Richards, A. Jain, G. Hautier, M. Kocher, S. Cholia, D. Gunter, V. L. Chevrier, K. A. Persson and G. Ceder, *Comput. Mater. Sci.*, 2013, **68**, 314-319.
11. Z. Deng, Z. Zhu, I.-H. Chu and S. P. Ong, *Chem. Mater.*, 2017, **29**, 281-288.
12. T. Croteau and G. N. Patey, *J. Chem. Phys.*, 2006, **124**, 244506.
13. G. E. Murch, *Solid State Ionics*, 1982, **7**, 177-198.
14. J. W. Liang, X. N. Li, S. Wang, K. R. Adair, W. H. Li, Y. Zhao, C. H. Wang, Y. F. Hu, L. Zhang, S. Q. Zhao, S. G. Lu, H. Huang, R. Y. Li, Y. F. Mo and X. L. Sun, *J. Am. Chem. Soc.*, 2020, **142**, 7012-7022.
15. X. N. Li, J. W. Liang, N. Chen, J. Luo, K. R. Adair, C. H. Wang, M. N. Banis, T.-K. Sham, L. Zhang, S. Q. Zhao, S. G. Lu, H. Huang, R. Y. Li and X. L. Sun, *Angew. Chem. Int. Ed. Engl.*, 2019, **58**, 16427-16432.
16. T. Asano, A. Sakai, S. Ouchi, M. Sakaida, A. Miyazaki and S. Hasegawa, *Adv. Mater.*, 2018, **30**, 1803075.
17. S. P. Ong, L. Wang, B. Kang and G. Ceder, *Chem. Mater.*, 2008, **20**, 1798-1807.
18. L. J. Miara, W. D. Richards, Y. E. Wang and G. Ceder, *Chem. Mater.*, 2015, **27**, 4040-4047.
19. T. T. Jia, G. Chen and Y. S. Zhang, *Phys. Rev. B*, 2017, **95**, 155206.